THE JOURNAL OF PHYSICAL CHEMISTRY Letters

pubs.acs.org/JPCL

High-Performance Scalable Molecular Dynamics Simulations of a Polarizable Force Field Based on Classical Drude Oscillators in NAMD

Wei Jiang,[†,△] David J. Hardy,[‡,△] James C. Phillips,[‡,△] Alexander D. MacKerell, Jr.,[*,¶] Klaus Schulten,[*,§,‡] and Benoît Roux[*,∥,⊥]

[†]Argonne Leadership Computing Facility, Argonne National Laboratory, Lemont, Illinois 60439, United States, [‡]Beckman Institute, University of Illinois at Urbana−Champaign, Urbana, Illinois 61801, United States, [¶]Department of Pharmaceutical Sciencies, School of Pharmacy, University of Maryland, Baltimore Maryland 21201, United States, [§]Department of Physics, University of Illinois at Urbana−Champaign, Urbana, Illinois 61801, United States, [∥]Department of Biochemistry and Molecular Biology, University of Chicago, Chicago, Illinois 60637, United States, and [⊥]Biosciences Division, Argonne National Laboratory, Argonne, Illinois 60439, United States

ABSTRACT Incorporating the influence of induced polarization in large-scale atomistic molecular dynamics (MD) simulations is a critical challenge in the progress toward computations of increased accuracy. One computationally efficient treatment is based on the classical Drude oscillator in which an auxiliary charged particle is attached by a spring to each nucleus. Here, we report the first implementation of this model in the program NAMD. An extended Lagrangian dynamics with a dual-Langevin thermostat scheme applied to the Drude−nucleus pairs is employed to efficiently generate classical dynamic propagation near the self-consistent field limit. Large-scale MD simulations based on the Drude polarizable force field scale very well on massively distributed supercomputing platforms, the computational demand increasing by only a factor of 1.2 to 1.8 compared to nonpolarizable models. As an illustration, a large-scale 150 mM NaCl aqueous salt solution is simulated, and the calculated ionic conductivity is shown to be in excellent agreement with experiment.

SECTION Molecular Structure, Quantum Chemistry, General Theory

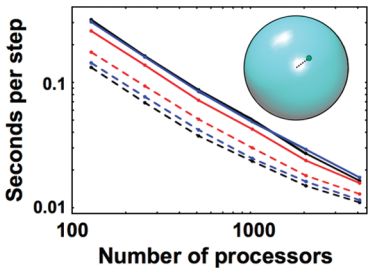

Most classical MD simulations employ potential functions that do not treat for many-body induced polarization effects explicitly.[1−4] Such simple potential functions, accounting for polarization in an average way using simple fixed effective partial charges, have been remarkably successful in modeling complex molecular systems. Nevertheless, such potential functions are clearly limited in their ability to provide a realistic and accurate representation of both microscopic and thermodynamic properties, particularly when induced electronic polarization is expected to play a significant role. In recent years, intensive efforts have been directed to the development of computational models able to account for induced polarization explicitly for the purpose of generating MD trajectories. Popular approaches include the induced dipole model,[5−7] the fluctuating charge model,[8−12] and the classical Drude oscillator model.[13−24]

While intense efforts have been and continue to be devoted to the careful parametrization of force fields based on various realizations of these models, their increased computational cost compared to that of nonpolarizable models is an issue that needs also to be addressed. For instance, simulations of large-scale systems (millions of atoms) are beyond the capabilities of the MD programs currently equipped to treat induced polarization. In addition to critical technical aspects encountered in large-scale simulations of nonpolarizable models, a number of factors can affect performance regarding the particular polarizable model chosen and its implementation. One particularly attractive feature of the Drude oscillator model, which represents induced electronic polarization by introducing an auxiliary particle attached to each polarizable atom via a harmonic spring, is that it preserves the simple particle−particle Coulomb electrostatic interaction employed in nonpolarizable force fields. For this reason, an implementation of the Drude model into a high-performance MD program is relatively straightforward. Furthermore, the auxiliary particles are attributed a finite mass and are bonded to the atoms. In principle, any latent "polarization catastrophe" can be controlled by modifying the Drude bond parameters, thus achieving high numerical stability. Thus, the auxiliary Drude particle can essentially be treated as any physical particle of the molecule of interest. These basic ingredients

Received Date: October 27, 2010
Accepted Date: December 20, 2010
Published on Web Date: December 23, 2010

DOI: 10.1021/jz101461d | *J. Phys. Chem. Lett.* 2011, 2, 87–92

were utilized to construct a polarizable water model called SWM4-NDP (simple water model with four sites and a negative Drude particle),[17] which was implemented and simulated with the program CHARMM.[25] Additional efforts are now aimed at the development of a complete polarizable force field for biomolecular simulations.[24]

In the present Letter, we report the first implementation of a polarizable force field based on the classical Drude oscillator model in the program NAMD.[26] NAMD is a parallel MD code designed for high-performance simulations of large-scale biomolecular systems based on nonpolarizable force fields.[26] NAMD adopts a seminal hybrid of force and spatial decomposition and therefore avoids the limitation of simulation space and poor load balance due to simple spatial decomposition. The high efficiency of NAMD and the simplicity of the Drude oscillator model offers a unique opportunity to achieve high performance in an implementation of induced polarization in large-scale MD simulations.

Implementation of the Drude model into NAMD was based on the following programming strategy. To avoid the computationally prohibitive self-consistent field (SCF) procedure, which is normally required to treat induced polarization, an extended Lagrangian with a dual-Langevin thermostat scheme applied to the Drude−nucleus pairs is developed. This enables the efficient generation of classical trajectories that are near the SCF limit. A series of test simulations of unprecedented large scale are carried out to evaluate both the accuracy and performance of the Drude implementation in NAMD. Several of the simulated systems have more than 150K atoms and are beyond the capabilities of other available MD packages permitting a treatment of induced polarization.

In a previous implementation of the Drude model, the extended Lagrangian was achieved by designing a dual energy-conserving Nosé−Hoover thermostat acting on, and within, each nucleus−Drude pair.[13] In the present implementation for NAMD, this is achieved via dual stochastic Langevin thermostats. A Langevin thermostatting scheme is advantageous for high-performance computing platforms because it can be implemented locally while avoiding the global communication of the kinetic temperature T^* required by a Nosé−Hoover scheme. Furthermore, a Langevin thermostatting scheme is extremely effective at equipartitioning energy, which confers a great dynamical stability in large-scale heterogeneous biomolecular systems. An alternative would be to use dual Lowe−Anderson thermostats,[27,28] which can also be implemented in NAMD with great efficiency. To achieve SCF-like dynamics, it is critical that the cold thermostats at temperature T^* act on the atom−Drude oscillator pairs rather than on the Drude particles directly.[13] The implementation is achieved by separating the dynamics of each atom−Drude pair with coordinates $\mathbf{r}_i$ and $\mathbf{r}_{D,i}$ in terms of the global motion of the center-of-mass $\mathbf{R}_i$ and the relative internal motion of the oscillator $\mathbf{d}_i = \mathbf{r}_{D,i} - \mathbf{r}_i$. Denoting m_i as the total mass of the pair, and $m_i' = m_D(1 - m_D/m_i)$ as the reduced mass of the oscillator, the equations of motion of the Drude−atom pair are

$$m_i\ddot{\mathbf{R}}_i = \mathbf{F}_{\mathbf{R},i} - \gamma\dot{\mathbf{R}}_i + \mathbf{f}_i \quad (1)$$

$$m_i'\ddot{\mathbf{d}}_i = \mathbf{F}_{\mathbf{d},i} - \gamma'\dot{\mathbf{d}}_i + \mathbf{f}_i' \quad (2)$$

where $\mathbf{F}_{\mathbf{R},i} = -\partial U/\partial\mathbf{R}_i$ and $\mathbf{F}_{\mathbf{d},i} = -\partial U/\partial\mathbf{d}_i$ are the forces acting on the center-of-mass and on the reduced mass, respectively. The coupling to dual heat baths is modeled by the addition of damping and noise terms, where γ and γ' are external and internal Langevin friction coefficients. The $\mathbf{f}_i$ and $\mathbf{f}_i'$ are time-dependent fluctuating random forces obeying the fluctuation−dissipation theorem, $\mathbf{f}_i = (2\gamma k_B T/m_i)^{1/2}R(t)$ and $\mathbf{f}_i'r = (2\gamma' k_B T^*/m_i')^{1/2}R^*(t)$, where $R(t)$ and $R^*(t)$ are univariate Gaussian random processes. The temperature T of the "physical" thermostat is chosen to keep the atoms at room temperature, while the temperature T^* is set to a small value in order to reduce the thermal fluctuation of the Drude oscillators. If T^* is set to 0, the thermostat on the oscillators is eliminated. For low values of T^*, the actual Drude oscillator temperature maintained by the thermostat will depend mostly on the balance between energy dissipated by the damping term and energy introduced by elecrostatic coupling to the environment. The forces on the centers-of-mass and on the displacements can be expressed in terms of the actual forces on the particles

$$\mathbf{F}_{\mathbf{R},i} = -\frac{\partial U}{\partial \mathbf{r}_i} - \frac{\partial U}{\partial \mathbf{r}_{D,i}} \quad (3)$$

$$\mathbf{F}_{\mathbf{d},i} = -\left(1 - \frac{m_D}{m_i}\right)\frac{\partial U}{\partial \mathbf{r}_{D,i}} + \left(\frac{m_D}{m_i}\right)\frac{\partial U}{\partial \mathbf{r}_i} \quad (4)$$

The Brünger−Brooks−Karplus (BBK) method,[29] a natural extension of the Verlet algorithm,[30,31] is used in NAMD to integrate the Langevin equation.[26] Extension of the atom-based Langevin equation to accommodate the dual thermostats for Drude oscillators requires very small modifications to the existing source code. Because the integration of the centers-of-mass and the displacements is identical to the integration of the individual atoms, except for the update of the velocities with the thermostats, NAMD treats the entire system as standard atomic coordinates until the application of the thermostats to velocities, at which point, an atom−Drude oscillator pair is transformed to center-of-mass and relative displacement coordinates, the respective thermostats are applied to the transformed coordinates, and the coordinates are transformed back to standard atomic coordinates. Independent of the Drude particle attached to the oxygen, the model also imposes a rigid geometry to the rigid four-site water model SWM4-NDP,[17] which is implemented via the Settle algorithm.[32] The implementation of the Drude model in NAMD utilizes the existing spatial decomposition into "patches" to retain scalable parallelism.[26] Each Drude particle must be kept in the same patch with its parent atom for the application of the thermostat to the Drude oscillator. Each massless lone pair and its three guide atoms must similarly be kept in the same patch.[18] Additional details of the implementation are included in the Supporting Information.

The ultimate purpose of implementating the Drude model in NAMD is to enable large-scale simulations on massively parallel supercomputers. Compared to the corresponding nonpolarizable model, the Drude model introduces not only new degrees of freedom but also a force redistribution for lone pairs. Making sure that these features do not decrease the

DOI: 10.1021/jz101461d | J. Phys. Chem. Lett. 2011, 2, 87–92

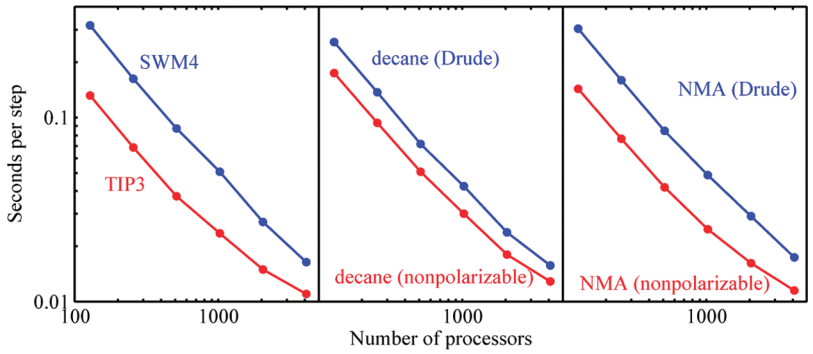

Figure 1. Scalability of NAMD with Drude models. Blue curves, Drude models; red curves, nonpolarizable models. Scaling performance tests were performed with systems comprising 72 000 water molecules, 8576 decane molecules, and 18 944 *N*-methylacetamide (NMA) molecules. The test systems were simulated under isothermal−isobaric (NPT) condition at 298.15 K. For each system, 20 000 steps of MD simulations were carried out for both the polarizable and nonpolarizable CHARMM force field (see Supporting Information for details). Note that the Drude models show excellent scaling up to 4096 processors, while nonpolarizable models exhibit weaker scalability.

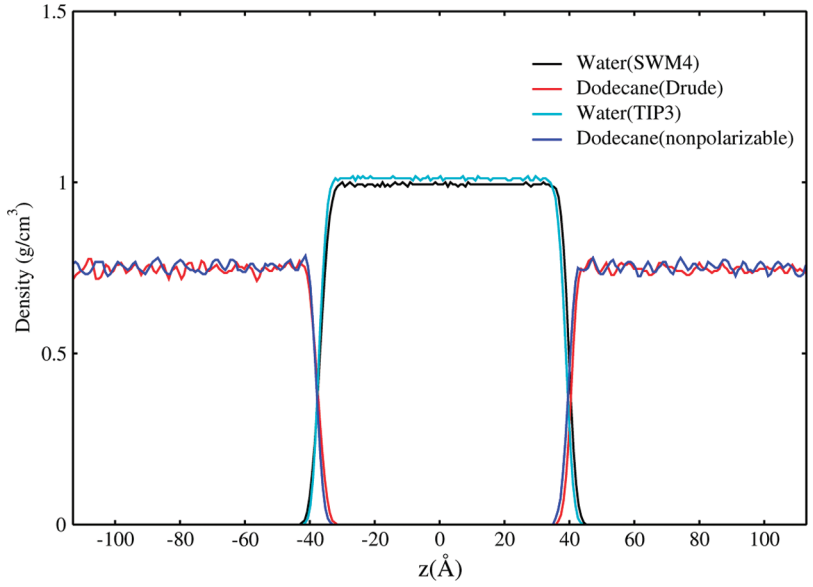

Figure 2. Surface-normal density profile of the water/dodecane liquid/liquid interface. Results from 10 ns MD simulations of a model of a water/dodecane liquid/liquid interface. The system was simulated at 298.15 K with periodic boundary conditions under NPT conditions with a constant area.

parallel performance of NAMD is crucial for large-scale simulations. Three basic systems that include all features of the Drude model were simulated, SWM4-NDP, decane, and NMA. Figure 1 shows the parallel performance of NAMD on Blue Gene/P for all three systems modeled with and without polarizability. For all three systems, the computations scale well to 4096 processors (1 standard Blue Gene/P rack). For the nonpolarizable model, linear scaling holds only up to 2048 processors due to the smaller number of particles that is known to limit linear scaling. The SWM4-NDP system exhibits the largest relative speed ratio between the Drude model and the nonpolarizable model, namely, 1:2. The relative speed ratio of decane is about 1:1.6, and NMA has a ratio of 1:1.8. These ratios demonstrate that the present implementation of the Drude model in NAMD is quite efficient, that is, that inclusion of Drude model atomic polarizability costs only up to 100% more computing effort.

Simulations of extensive liquid/liquid interfaces are challenging. The electronic polarization often plays a significant role, and a large simulation size is necessary to eliminate finite-size effects. Figure 2 shows the normal density profiles of a water/dodecane interface composed of 16 000 water molecules and 1280 dodecane molecules. Both the Drude and nonpolarizable models give satisfactory density profiles for water and dodecane. However, the Drude model results in a bulk water density of 0.997 ± 0.001 g/cm^3, closer to the experimental value of 0.997 g/cm^3 than the nonpolarizable model value of 1.01 ± 0.001 g/cm^3. For dodecane, both models give an excellent bulk density (0.75 ± 0.004 g/cm^3), the agreement between the models being most likely due to the weak polarity of alkane species. Accuracy of the surface tension is an important aspect of the quality of a molecular force field. Compared to the experimental value of 53.7 dyn/cm,[33] the surface tension from the Drude model

DOI: 10.1021/jz101461d | *J. Phys. Chem. Lett.* **2011**, *2*, 87–92

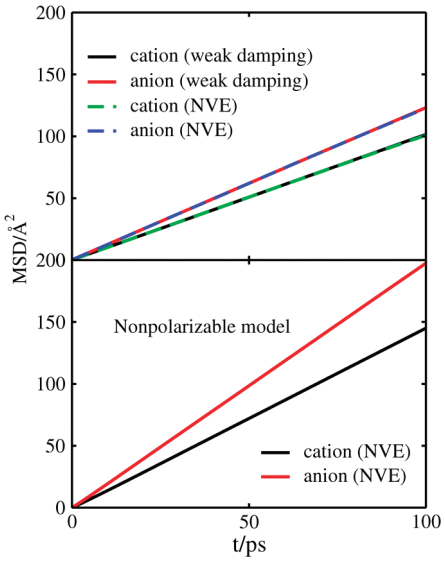

Figure 3. Time evolution of mean-squared displacements (MSDs) of ions. Upper panel, Drude models; lower panel, nonpolarizable models. In the case of the Drude model, NVE and NVT simulations with weak Langevin damping coefficients result in identical diffusive behaviors. (i.e., the upper panel plots overlap for the cation and anion, respectively).

(49 ± 2 dyn/cm) is slightly better than that from the nonpolarizable model (46 ± 2 dyn/cm). Liquid/air interface simulations of 5 ns were also performed for water/air and dodecane/air interfaces with Drude models. The resultant surface tensions are 67 ± 2 (CHARMM result, 67 dyn/cm) and 26 ± 2 dyn/cm, respectively, in agreement with respective experimental values of 72 and 25.3 dyn/cm.[33]

As a last illustration of the present implementation, we consider the simulation of the NaCl aqueous solution at a concentration of 150 mM. Such a system represents the salt concentration in the extracellular plasma, which is of great interest for physiology and medicine. It turns out that achieving a quantitative characterization of the transport properties of such a system with MD simulations based on polarizable models stands as a particularly challenging problem. Realistic atomic models require a very large number of ion pairs to properly account for ion−ion correlation and to avoid spurious finite-size effects, which leads to extremely large simulation systems. While such simulations could be executed without huge problems in the case of nonpolarizable models, the task rapidly exceeds the ability of current MD simulation programs in the case of polarizable models.[34]

To address this challenge, a large-scale model of the NaCl aqueous salt solution at 150 mM was simulated. The atomic model was comprised of 172 Na^+ and Cl^- pairs and 63 656 water molecules based on the rigid four-site SWM4-NDP[17] model, with the ions described as those in Yu et al.[35] The parameters of the ions were optimized based on the properties of small hydrated clusters that include one ion and a few water molecules to account for the thermodynamics of ion hydration at infinite dilution. Interestingly, the ability of polarizable models to represent ionic solutions at finite concentration remains untested, and the present simulation provides the first data in this regard. A dual Langevin multiple time step integration scheme was employed for the polarizable Drude model, with time steps of 0.5 fs for the bonded calculations and 1.0 fs for nonbonded and long-range calculations, respectively. This is necessary for stable integration of the anharmonic restoring force introduced to prevent large excursions of the Drude particle of the anions at finite concentrations.[35] As a comparison, a nonpolarizable model was also simulated. Additional details are provide in Supporting Information.

Figure 3 shows the mean-squared displacement (MSD) of ions described through Drude and nonpolariable models. To validate the application of weak Langevin damping for the simulations, an NVE simulation without any Langevin dissipation was performed for the Drude model. The NVE and NVT simulations with weak Langevin damping result in essentially identical diffusive behaviors for the ions; the diffusion constants for the Drude cation and anion are $(1.69 \pm 0.02) \times 10^{-9}$ and $(2.06 \pm 0.02) \times 10^{-9}$ m^2/s, respectively, close to the experimental values (cation 1.33×10^{-9} m^2/s and anion 1.67×10^{-9} m^2/s) at infinite dilute solution.[36] In contrast, the diffusion constants of the nonpolarizable model are $(2.41 \pm 0.02) \times 10^{-9}$ and $(3.29 \pm 0.02) \times 10^{-9}$ m^2/s. The conductivity was calculated from the center-of-charge diffusion eq 5 and the total flux−flux autocorrelation function eq 6

$$\sigma = \lim_{t \to \infty} \frac{e^2}{6tVk_BT} \sum_{ij}^{N} z_i z_j \langle [\mathbf{R}_i(t) - \mathbf{R}_i(0)] \cdot [\mathbf{R}_j(t) - \mathbf{R}_j(0)] \rangle \tag{5}$$

$$\sigma = \frac{e^2}{3Vk_BT} \int_0^\infty dt \langle \left[\sum_i \mathbf{V}_{i^+}(t) - \sum_j \mathbf{V}_{j^-}(t) \right] \left[\sum_i \mathbf{V}_{i^+}(0) - \sum_j \mathbf{V}_{j^-}(0) \right] \rangle \tag{6}$$

where z_i denotes the charge of an ion, $\mathbf{R}_i$ denotes the coordinate, and $\mathbf{V}_{i^{+(-)}}$ denotes the velocity of cations (anions). Figure 4 shows the MSDs of ion charge and the corresponding flux autocorrelation functions (inset). The conductivities calculated from the center-of-charge diffusion is 17.3 ± 0.5 (Drude model) and 28.2 ± 0.4 mS/cm (nonpolarizable model). Correspondingly, the conductivities calculated from the flux−flux autocorrelation function are 14.7 ± 1.0 and 24.4 ± 1.0 mS/cm. The difference in the results from these two routes can be attributed to the error in numerical integration. Those results can be compared to the experimental value of 16 mS/cm.[37] Interestingly, the flux autocorrelation function of the nonpolarizable model exhibits fairly strong oscillations at short times (around 0.1 ps), which are the signature of back scattering due to caging effects in the liquid. The corresponding oscillations are considerably smaller for the polarizable model, most likely because the inclusion of induced polarization facilitates the local relaxation of molecular dipoles, thus decreasing caging effects. The impact of ion−ion correlations can be further highlighted by considering the Nernst−Einstein relation, which estimates the

DOI: 10.1021/jz101461d | J. Phys. Chem. Lett. 2011, 2, 87–92

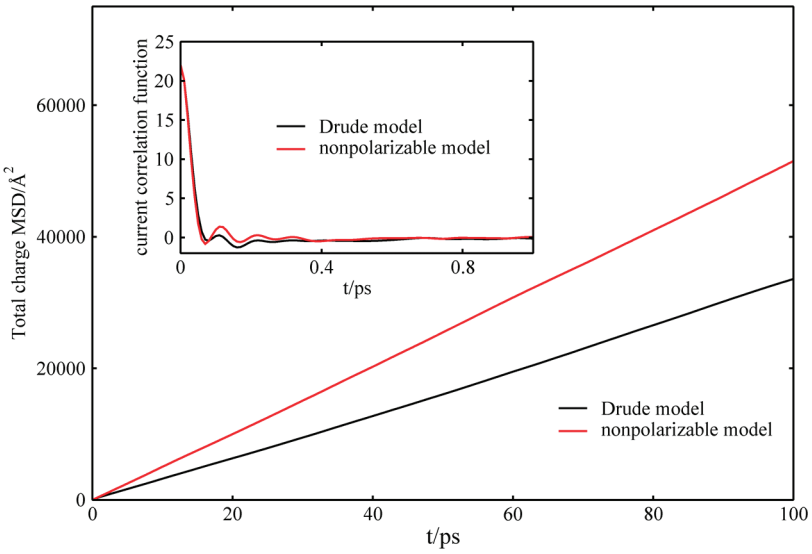

Figure 4. Time evolution of total charge MSDs and total ion current autocorrelation functions. Inset, total ion autocorrelation functions, calculated from 5 ns MD simulations performed at 298.15 K under NVT conditions with weak Langevin damping for both the polarizable and nonpolarizable force fields.

conductivity to be

$$\sigma = \frac{Ne^2}{Vk_BT}(D_+ + D_-) \quad (7)$$

where D_+ and D_- denote the self-diffusion coefficient of the cations and anions, respectively. This expression neglects the cross-correlations between ions, which are included in the expression for the center-of-charge diffusion eq 6. Using eq 7, the conductivities of the Drude and nonpolarizable models is 20.4 ± 0.3 and 32.4 ± 0.4 mS/cm, respectively. The deviation from the results stated above indicate that ion−ion correlations are not negligible, even at physiological concentration. It is worth noting that the Nernst−Einstein approximation appears to yield a more accurate result for the polarizable Drude model, suggesting that dynamical ion−ion correlations are considerably enhanced in the nonpolarizable model. This is perhaps due to the lack of electrostatic shielding by the induced dipoles.

In conclusion, the first implementation of a polarizable force field in the high-performance scalable MD simulation program NAMD was presented. The force field is based on the classical Drude oscillator, which preserves the outstanding scalability of NAMD. Test simulations demonstrate that the present implementation is numerically stable, yielding results consistent with previous results calculated using CHARMM. As an illustration, a simulation of a physiological aqueous salt solution was performed, and the calculated conductivity was shown to be in excellent agreement with that from experiment. The present strategy should be applicable to general all-atom, large-scale simulations. Simulations of proteins, membranes, and nucleic acids based on the Drude polarizable force field with NAMD are currently underway.

SUPPORTING INFORMATION AVAILABLE Further details regarding the polarizable force field based on classical Drude oscillators, decomposition strategy of nonbonded interaction and simulation systems, and computational details. This material is available free of charge via the Internet at http://pubs.acs.org.

AUTHOR INFORMATION

Corresponding Author:

*To whom correspondence should be addressed. E-mail: alex@outerbanks.umaryland.edu (A.D.M.); kschulte@ks.uiuc.edu (K.S.); roux@uchicago.edu (B.R.).

Author Contributions:

△ These authors contributed equally.

ACKNOWLEDGMENT We are grateful to Ray Loy for his help building the CVS version of NAMD on Blue Gene/P Intrepid. The work of W.J. is supported by the Computational Postdoctoral Fellowship from the Argonne Leadership Computing Facility (ALCF). The work of B.R. and A.D.M. is supported by the National Institutes of Health through Grants GM072558, GM070855, and GM051501. The work of D.H., J.P., and K.S. is supported by the National Institutes of Health through Grant P41-RR005969. This research used resources of the Argonne Leadership Computing Facility (ALCF) at Argonne National Laboratory, which is supported by the Office of Science of the U.S. Department of Energy (DOE) under contract DE-AC02-06CH11357. The submitted manuscript has been created by UChicago Argonne, LLC, Operator of Argonne National Laboratory ("Argonne"). The U.S. Government retains for itself, and others acting on its behalf, a paid-up nonexclusive, irrevocable worldwide license in said article to reproduce, prepare derivative works, distribute copies to the public, and perform publicly and display publicly, by or on behalf of the Government.

REFERENCES

(1) Cornell, W.; Cieplak, P.; Bayly, C.; Gould, I., Jr.; K., M.; Ferguson, D.; Spellmeyer, D.; Fox, T.; Caldwell, J.; Kollman, P. A Second Generation Force Field for the Simulation of Proteins and Nucleic Acids. *J. Am. Chem. Soc.* **1995,** *117*, 5179–5197.

DOI: 10.1021/jz101461d | *J. Phys. Chem. Lett.* **2011**, *2*, 87–92

(2) MacKerell, A. D., Jr.; et al. All-Hydrogen Empirical Potential for Molecular Modeling and Dynamics Studies of Proteins Using the CHARMM22 Force Field. *J. Phys. Chem. B* **1998,** *102*, 3586–3616.
(3) Hermans, J.; Berendsen, H.; van Gunsteren, W.; Postma, J. A Consistent Empirical Potential for Water-Protein Interactions. *Biopolymers* **1984,** *23*, 1513–1518.
(4) Jorgensen, W. L.; Tirado-Rives, J. The OPLS Potential Functions for Proteins. Energy Minimization for Crystal of Cyclic Peptides and Crambin. *J. Am. Chem. Soc.* **1988,** *110*, 1657–1666.
(5) Caldwell, J. W.; Kollman, P. A. Structure and Properties of Neat Liquids Using Nonadditive Molecular Dynamics: Water, Methanol, and *N*-Methylacetamide. *J. Phys. Chem.* **1995,** *99*, 6208–6219.
(6) Cieplak, P.; Caldwell, J.; Kollman, P. Molecular Mechanical Models for Organic and Biological Systems Going Beyond the Atom Centered Two Body Additive Approximation: Aqueous Solution Free Energies of Methanol and *N*-Methyl Acetamide, Nucleic Acid Base, and Amide Hydrogen Bonding and Chloroform/Water Partition Coefficients of the Nucleic Acid Bases. *J. Comput. Chem.* **2001,** *22*, 1048–1057.
(7) Kaminski, G.; Friesner, R. A.; Zhou, R. A Computationally Inexpensive Modification of the Point Dipole Electrostatic Polarization Model for Molecular Simulations. *J. Comput. Chem.* **2003,** *24*, 267–276.
(8) Rick, S. W.; Stuart, S. J.; Bader, J. S.; Berne, B. J. Fluctuating Charge Force Fields for Aqueous Solutions. *J. Mol. Liq.* **1995,** *66*, 31–40.
(9) Rick, S. W.; Berne, B. J. Dynamical Fluctuating Charge Force Fields: The Aqueous Solvation of Amides. *J. Am. Chem. Soc.* **1996,** *118*, 672–679.
(10) Rick, S. W.; Stuart, S. J.; Berne, B. J. Dynamical Fluctuating Charge Force Field: Application to Liquid Water. *J. Chem. Phys.* **1994,** *101*, 6141–6156.
(11) Stern, H. A.; Rittner, F.; Berne, B. J.; Friesner, R. A. Combined Fluctuating Charge and Polarizable Dipole Models: Application to a Five-Site Water Potential Function. *J. Chem. Phys.* **2001,** *115*, 2237–2251.
(12) Rick, S. W. Simulations of Ice and Liquid Water over a Range of Temperatures Using the Fluctuating Charge Model. *J. Chem. Phys.* **2001,** *114*, 2276–2283.
(13) Lamoureux, G.; Roux, B. Modeling Induced Polarization with Classical Drude Oscillators: Theory and Molecular Dynamics Simulation Algorithm. *J. Chem. Phys.* **2003,** *119*, 3025–3039.
(14) Lamoureux, G.; MacKerell, A. D., Jr.; Roux, B. A Simple Polarizable Model of Water Based on Classical Drude Oscillators. *J. Chem. Phys.* **2003,** *119*, 5185–5197.
(15) Anisimov, V. M.; Lamoureux, G.; Vorobyov, I. V.; Huang, N.; Roux, B.; MacKerell, A. D., Jr. Determination of Electrostatic Parameters for a Polarizable Force Field Based on the Classical Drude Oscillator. *J. Chem. Theory Comput.* **2005,** *1*, 153–168.
(16) Vorobyov, I. V.; Anisimov, V. M.; MacKerell, A. D., Jr. Polarizable Empirical Force Field for Alkanes Based on the Classical Drude Oscillator Model. *J. Phys. Chem. B* **2005,** *109*, 18988–18999.
(17) Lamoureux, G.; Harder, E.; Vorobyov, I. V.; Roux, B.; MacKerell, A. D., Jr. A Polarizable Model of Water for Molecular Dynamics Simulations of Biomolecules. *Chem. Phys. Lett.* **2006,** *418*, 245–249.
(18) Harder, E.; Anisimov, V. M.; Vorobyov, I. V.; Lopes, P. E. M.; Noskov, S. Y.; MacKerell, A. D., Jr.; Roux, B. Atomic Level Anisotropy in the Electrostatic Modeling of Lone Pairs for a Polarizable Force Field Based on the Classical Drude Oscillator. *J. Chem. Theory Comput.* **2006,** *2*, 1587–1597.
(19) Anisimov, V. M.; Vorobyov, I. V.; Roux, B.; MacKerell, A. D., Jr. Polarizable Empirical Force Field for the Primary and Secondary Alcohol Series Based on the Classical Drude Model. *J. Chem. Theory Comput.* **2007,** *3*, 1927–1946.
(20) Lopes, P. E. M.; Lamoureux, G.; Roux, B.; MacKerell, A. D., Jr. Polarizable Empirical Force Field for Aromatic Compounds Based on the Classical Drude Oscillator. *J. Phys. Chemw. B* **2007,** *111*, 2873–2885.
(21) Vorobyov, I.; Anisimov, V. M.; Greene, S.; Venable, R. M.; Moser, A.; Pastor, R. W.; MacKerell, A. D., Jr. Additive and Classical Drude Polarizable Force Fields for Linear and Cyclic Ethers. *J. Chem. Theory Comput.* **2007,** *3*, 1120–1133.
(22) Whitfield, T. W.; Varma, S.; Harder, E.; Lamoureux, G.; Rempe, S. B.; Roux, B. Theoretical Study of Aqueous Solvation of K^+ Comparing Ab Initio, Polarizable, and Fixed-Charge Models. *J. Chem. Theory Comput.* **2007,** *3*, 2068–2082.
(23) Harder, E.; Anisimov, V. M.; Whitfield, T. W.; MacKerell, A. D., Jr.; Roux, B. Understanding the Dielectric Properties of Liquid Amides from a Polarizable Force Field. *J. Phys. Chem. B* **2008,** *112*, 3509–3521.
(24) Lopes, P. E.; Roux, B.; MacKerell, A. D., Jr. Molecular Modeling and Dynamics Studies with Explicit Inclusion of Electronic Polarizability. Theory and Applications. *Theor. Chem. Acc.* **2009,** *124*, 11–28.
(25) Brooks, B. R.; et al. CHARMM: The Biomolecular Simulation Program. *J. Comput. Chem.* **2009,** *30*, 1545–1614.
(26) Phillips, J.; Braun, R.; Wang, W.; Gumbart, J.; Tajkhorshid, E.; Villa, E.; Chipot, C.; Skeel, R.; Kale, L.; Schulten, K. Scalable Molecular Dynamics with NAMD. *J. Comput. Chem.* **2005,** *26*, 1781.
(27) Lowe, C. An Alternative Approach to Dissipative Particle Dynamics. *Europhys. Lett.* **1999,** *47*, 145–151.
(28) Koopman, E. A.; Lowe, C. P. Advantages of a Lowe—Andersen Thermostat in Molecular Dynamics Simulations. *J. Chem. Phys.* **2006,** *124*, 204103.
(29) Bruenger, A.; Brooks, C. B.; Karplus, M. Stochastic Boundary Conditions for Molecular Dynamics Simulations of ST2 Water. *Chem. Phys. Lett.* **1984,** *105*, 495–500.
(30) Verlet, L. Computer Experiments on Classical Fluids. I. Thermodynamical Properties of Lennard-Jones Molecules. *Phys. Rev.* **1967,** *159*, 98–103.
(31) Verlet, L. Computer Experiments on Classical Fluids. II. Equilibrium Correlation Functions. *Phys. Rev.* **1968,** *165*, 201–214.
(32) Miyamoto, S.; Kollman, P. SETTLE: An Analytical Version of the SHAKE and RATTLE Algorithm for Rigid Water Models. *J. Comput. Chem.* **1992,** *13*, 952–962.
(33) Goebel, A.; Lunkenheimer, K. Interfacial Tension of the Water/*N*-Alkane Interface. *Langmuir* **1997,** *13*, 369–372.
(34) Ponder, J.; Wu, C.; Ren, P.; Pande, V.; Chodera, J.; Schnieders, M.; Haque, I.; Mobley, D.; Lambrecht, D.; DiStasio, R., Jr.; et al. Current Status of the AMOEBA Polarizable Force Field. *J. Phys. Chem. B* **2010,** *114*, 2549–2564.
(35) Yu, H.; Whitfield, T.; Harder, E.; Lamoureux, G.; Vorobyov, I.; Anisimov, V.; MacKerell, A. D., Jr.; Roux, B. Simulating Monovalent and Divalent Ions in Aqueous Solution Using a Drude Polarizable Force Field. *J. Chem. Theory Comput.* **2010,** *6*, 774–786.
(36) Lide, D. R., Ed. *CRC Handbook of Chemistry and Physics*, 87th ed.; Taylor and Francis: Boca Raton, FL, 2007.
(37) Robinson, R.; Stokes, R. *Electrolyte Solutions*; Dover Publications: Mineola, NY, 2002.

DOI: 10.1021/jz101461d | *J. Phys. Chem. Lett.* **2011,** *2*, 87–92